Energy Harvesting-based Multicast communication in Cellular IoT

Abdullah M. Almasoud and Ahmed E. Kamal,
Department of Electrical and Computer Engineering, Iowa State University, Ames, IA 50011, USA,
E-mails: {almasoud, kamal}@iastate.edu.

***Abstract*—Internet of Things (IoT) is a promising technology that enables interconnecting billions of electronic devices over communication networks. Multicasting is an essential service in IoT which allows the IoT devices to disseminate common messages more efficiently. Energy consumption is one of the main concerns in designing and implementing IoT since the IoT devices are expected to run for long periods of time using batteries in general. Moreover, IoT devices that participate in forwarding multicast messages excessively may deplete their energy sooner than expected. In this paper, we proposed to employ Radio Frequency (RF) energy harvesting technology with the IoT device in order to wirelessly power multicast sessions. Each IoT device that forwards a multicast message is compensated for the energy consumed for transmission by energy transmitted from Energy Transmitters (ETs).**

We formulate an optimal operational strategy, where the objective is to minimize the total transmitted energy from the ETs. The problem is in the form of non-convex Mixed Integer Nonlinear Problem, where there is no efficient way to solve the problem optimally when the number of variables is relatively large. Therefore, we first approximate the data rate function with a concave lower bound function. Then, we decompose the optimization problem using Generalized Bender Decomposition (GBD) into: 1) Convex Nonlinear Program (NLP) and 2) Mixed Integer Linear Program (MILP). Moreover, we employ Successive Convex Programming (SCP) within GBD algorithm to iteratively find a better approximation for the original problem. Our simulation results show that GBD-SCP algorithm solves the optimization problem more efficiently with a performance close to optimal.

***Index Terms*—Energy harvesting, power transfer, IoT, multicast, routing, scheduling.**

I. Introduction

In past few years, the data demand has increased rapidly due to the increase in the number of users in cellular networks and their applications. Multicast service in cellular networks is an essential service, and it is expected that applications demand for this service will increase further [1]. Multicast service in cellular networks are typically designed for human applications such as video content delivery. However, future cellular networks will incorporate a huge number of small Internet of Things (IoT) [2] devices that require supporting multicast service as well.

IoT is a technology that enables electronic devices to observe the surrounding environment, collect data and process it and then react accordingly to perform a designated task [2]. IoT devices in general are small devices equipped with limited batteries to run for a long period of time. Therefore, these small devices need to manage their energy consumption efficiently to prolong their battery lifetimes and to avoid the cost of batteries replacement. IoT devices involvement in excessive multicast messages forwarding may deplete their batteries early. Moreover, IoT devices may behave in selfish ways to avoid collaborating with other IoT devices in forwarding the multicast messages to prolong their battery lifetimes. Therefore, we address these challenges in this paper to encourage the IoT devices to collaborate while supporting their energy demand.

The authors in [3] proposed to use dedicated energy transmitters since harvesting energy from the ambient energy resource may not be sufficient. In [4], we proposed to use a cognitive mobile base station to transmit data and energy to the IoT such that we minimize the total consumed energy in mobility and energy transfer. Moreover, the authors in [6] proposed to utilize wireless energy transfer in cellular IoT where the goals are enhancing energy and spectrum utilization. In this paper, we propose energy harvesting-based multicast communication for IoT devices in cellular networks. To incentivize the IoT devices to participate in forwarding multicast messages, they receive Radio Frequency (RF) energy transmitted wirelessly from Energy Transmitters (ETs) to compensate for the energy consumed in multicasting. The goal is to minimize the total transmitted energy from the ETs such that multicast service for IoT devices is wirelessly powered.

We organize this paper as follows. We describe the system model in Section II, then we show how we formulate the optimization problem in Section III. We propose a solution for the optimization problem using GBD-SCP algorithm in Section IV. Moreover, we present and discuss the simulation results in Section V, then we conclude the paper in Section VI.

II. System Model

We consider a set of IoT devices, S, that can transmit multicast messages over a set of channels, C. These channels are assigned to a group of regular cellular users, P, for uplink transmission. The IoT devices transmits multicast messages underlaying the uplink band of a cellular network. Therefore, the IoT devices must keep their interference to the cellular users below a threshold Γ. Forwarding multicast messages can be in a form of multi-hop communication with Base Station (BS) assistance if needed. We name the set of all IoT devices and the BS $\overline{S}$.

To incentivize the IoT devices to collaborate in forwarding multicast messages, all IoT devices that consume energy for multicast message transmissions will be compensated by energy transmitted wirelessly from a set of Energy Transmitters (ETS). We assume that the IoT devices operate under harvest-use-store mode [5], where they harvest energy and use it, and only the remaining energy is saved in their batteries for future

use. Each Energy Transmitter (ET) can transfer energy to a group of IoT devices located within its energy harvesting zone over a set of channels, $\overline{C}$. We assume that time is slotted into $|Z|$ slot, where Z is the set of time slots and T is the duration of each slot.

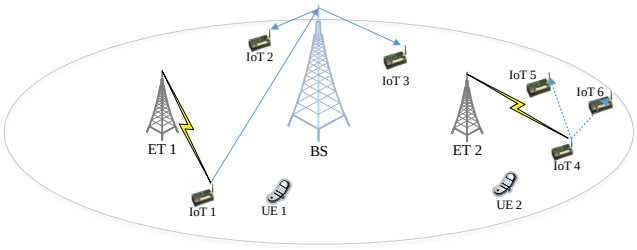

Fig. 1: Transmitted energy vs number of ETs.

Fig. 1 shows a scenario where IoT 1 transmits a multicast message to IoT 2 and IoT 3. The base station receives the multicast message from IoT 1 and forwards it to the destination IoT devices (i.e. IoT 2 and IoT 3). On the other hand, IoT 4 sends its multicast message directly to the destinations, which are IoT 5 and IoT 6. ET 1 and ET 2 transmit energy to IoT 1 and IoT 4, respectively, to compensate them for the energy consumed in the multicast messages transmissions. IoT 1 and IoT 4 need to keep their interference to the transmissions of the regular cellular users (i.e. UE 1 and UE 2) under a certain threshold, Γ^{cell}.

We assume that each IoT device is equipped with a single radio. Let PL_c be the path loss constant for channel c, PL_e be the path loss exponent, α_c and β_c be fast and slow fading gains for channel c, respectively, A_t and A_r be transmitting and receiving antenna gains, respectively, and d_{ij} be the distance between node i and node j. Hence, we can calculate the gain of channel c between node i and node j as follows:

$$G^c_{ij} = PL_c \ \alpha_c \ \beta_c \ A_t \ A_r \ d_{ij}^{-PL_e} \tag{1}$$

For IoT devices, we consider omnidirectional antennas where $A_t = A_r = 1$. On the other hand, ET uses directional antennas with antenna azimuth angles ϕ and elevation angles $\overline{\phi}$, in degree. Therefore, we can approximate A_t by [7]

$$A_t \approx \frac{30,000}{\phi \ \overline{\phi}} \tag{2}$$

Let $P^{tx}_i(c,z)$ be the transmission power of IoT device i over channel c and during time slot z. Hence, the signal to noise plus interference ratio for the signal transmitted by IoT device i and received by IoT device j over channel c and during slot z is given by

$$\gamma_{ij}(c,z) = \frac{P^{tx}_i(c,z) \ G^c_{ij}}{\sum_{q \in S \setminus i} P^{tx}_q(c,z) \ G^c_{qj} + N_j}. \tag{3}$$

where $N_j = \sum_{r \in P} P^{cell}_r(c,z) \ G^c_{rj} + N_0 W$ and $P^{cell}_r(c,z)$ is transmission power of the r^{th} cellular users to the BS over channel c and during slot z, N_0 is the noise spectral density and W is the channel bandwidth. Accordingly, we can calculate the data rate of the transmission from IoT device i to IoT device j over channel c and during time slot z as follows:

$$R_{ij}(c,z) = W \ \log_2\Big(1 + \gamma_{ij}(c,z)\Big) \tag{4}$$

We define a binary indicator function $\mathbb{H}^c_{ei}$ which equals one when IoT device i is located within the energy harvesting zone of the e^{th} ET, ET_e, that transfer energy over channel c. Thus, $\mathbb{H}^c_{ei}$ is defined as follows:

$$\mathbb{H}^c_{ei} = \begin{cases} 1, & d_{ei} \leq \left(\frac{P^{ET}_{max} PL_c \ \alpha_c \ \beta_c \ A_t \ A_r}{\Gamma^{EH}}\right)^{\frac{1}{PL_e}} \\ 0, & \text{otherwise.} \end{cases} \tag{5}$$

where P^{ET}_{max} is maximum transmission power for each ET and Γ^{EH} is energy harvesting threshold for minimum input power that enables the IoT device to harvest energy.

III. Problem Formulation

Let $X_i(c,z)$ and $H_i(c,z)$ be binary variables equal one only if IoT device i transmits data or harvest energy, respectively, over channel c and during slot z. Similarly, the binary variables $X_{ij}(c,z)$ and $H_{ei}(c,z)$ equal one only if IoT device i transmits data to a receiver j or harvest energy from ET_e, respectively, over channel c and during slot z. Since we assumed that the IoT device has a single radio, it can only transmit, receive or harvest energy at a time. Therefore,

$$\sum_{c \in C} \big[X_i(c,z) + \sum_{\forall k \in \overline{S}} X_{ki}(c,z)\big] + \sum_{c \in \overline{C}} H_i(c,z) \leq 1, \quad \forall i \in S, z \in Z. \tag{6}$$

Let $f^y_{ij}(c,z)$ be a variable representing the data flow destined for destination $y \in d$, in bits, from transmitter i to receiver j over channel c and during slot z. Hence, $X_{ij}(c,z)$ equals one only if there is a data flow from i to j over channel c and during slot z, i.e. $0 < f^y_{ij}(c,z)$. Therefore, we have the following:

$$X_{ij}(c,z) \leq \sum_{y=1}^{|d|} f^y_{ij}(c,z), \ \forall i \in S, j \in \overline{S}, \forall c \in C, z \in Z. \tag{7}$$

$$\frac{f^y_{ij}(c,z)}{v} \leq X_{ij}(c,z), \ \forall i \in S, j \in \overline{S}, c \in C, y \in d, z \in Z. \tag{8}$$

where v is the multicast message size, in bits.

Since the solutions of $X_i(c,z)$ and $X_{ij}(c,z)$ depend on each other, $X_i(c,z)$ equals one only if $\exists \ X_{ij}(c,z) = 1$. Thus, we have

$$X_i(c,z) \leq \sum_{j \in \overline{S}} X_{ij}(c,z), \ \forall i \in S, c \in C, z \in Z. \tag{9}$$

and

$$\frac{\sum_{j \in \overline{S}} X_{ij}(c,z)}{|\overline{S}|} \leq X_i(c,z), \forall i \in S, c \in C, z \in Z. \tag{10}$$

Similarly for $H_i(c,z)$, we have the following:

$$H_i(c,z) \leq \sum_{e \in ETS} H_{ei}(c,z), \ \forall i \in S, c \in \overline{C}, z \in Z. \tag{11}$$

$$\frac{\sum_{e \in ETS} H_{ei}(c,z)}{|ETS|} \leq H_i(c,z), i \in S, c \in \overline{C}, z \in Z. \tag{12}$$

Let Γ be a signal strength threshold for successful reception of a signal. Hence, $\gamma_{ij}(c,z)$ is lower bounded by Γ as follows:

$$\Gamma X_{ij}(c,z) \leq \gamma_{ij}(c,z), \ \forall i \in S, j \in \overline{S}, c \in C, z \in Z. \tag{13}$$

The flow over each link cannot be greater that the maximum number of bits that can be transmitted. Therefore,

$$f^y_{ij}(c,z) \leq R_{ij}(c,z)T, \ \forall i \in S, j \in \overline{S}, y \in d, c \in C, z \in Z. \tag{14}$$

Transmission power of the IoT device is zero when it is not transmitting, i.e.,

$$P^{tx}_i(c,z) \leq P^{tx}_{max} X_i(c,z), \quad \forall i \in S, c \in C, z \in Z. \tag{15}$$

where P_{max} is the maximum transmission power.

To route a multicast message of size v bits from a source s to a set of destination d, we have

$$\sum_{z=1}^{|Z|}\sum_{c\in C}\sum_{i\in\overline{S}\setminus s} f_{is}^{y}(c,z)=0,\quad \forall y\in d. \tag{16}$$

$$\sum_{z=1}^{|Z|}\sum_{c\in C}\sum_{j\in\overline{S}\setminus y} f_{yj}^{y}(c,z)=0,\quad \forall y\in d. \tag{17}$$

$$\sum_{z=1}^{|Z|}\sum_{c\in C}\sum_{j\in\overline{S}\setminus s} f_{sj}^{y}(c,z)=v,\quad \forall y\in d. \tag{18}$$

$$\sum_{z=1}^{|Z|}\sum_{c\in C}\sum_{i\in\overline{S}\setminus y} f_{iy}^{y}(c,z)=v,\quad \forall y\in d. \tag{19}$$

and

$$\sum_{z=1}^{|Z|}\sum_{c\in C}\sum_{n\in\overline{S}\setminus y} f_{ni}^{y}(c,z)=\sum_{z=1}^{|Z|}\sum_{c\in C}\sum_{j\in\overline{S}\setminus s} f_{ij}^{y}(c,z),\quad \forall i\in\overline{S}\setminus(s\cup y),\forall y\in d. \tag{20}$$

where flow bifurcation is allowed.

The IoT device must avoid causing harmful interference to the transmissions of the regular cellular users. Therefore,

$$\Gamma^{cell}\ X_k^{cell}(c,z)\le\frac{P_k^{cell}(c,z)G_{kb}^{c}}{\sum_{i\in S}P_i^{tx}(c,z)\ G_{ib}^{c}+N_0W}\quad \forall k\in P,c\in C,z\in Z. \tag{21}$$

where Γ^{cell} is a threshold of the maximum allowable interference to the regular cellular users and $X_k^{cell}(c,z)$ is a parameter equals one when the regular cellular user k transmits to the BS over channel c and at time slot z and zero otherwise.

Let $E_i^{tx}(z)$ and $E_i^{H}(z)$ be the total energy consumed and harvested by IoT i during slot z, respectively, which are given by

$$E_i^{tx}(z)=\sum_{c\in C}P_i^{tx}(c,z)T. \tag{22}$$

and

$$E_i^{H}(z)=\sum_{c\in\overline{C}}\sum_{k\in ETS}T\eta P_{ki}^{ET}(c,z)G_{ki}^{c}. \tag{23}$$

where $P_{ki}^{ET}(c,z)$ is the transmission power of ET_k to IoT device i over channel c and during slot z, and η is energy harvesting efficiency. Moreover, $P_{ei}^{ET}(c,z)$ equals zero if the IoT device i is not scheduled for receiving energy from ET_e over channel c and during slot z. Hence,

$$P_{ei}^{ET}(c,z)\le P_{max}^{ET}H_{ei}(c,z),\quad \forall e\in ETS,\forall i\in S,\forall c\in C,z\in Z. \tag{24}$$

To incentivize IoT devices to forward the multicast message, ETs send amount of energy to each IoT participating in forwarding the multicast message such that the total received energy is not less than the total consumed energy in multicast message transmission, i.e.,

$$\sum_{z=1}^{|I|}E_i^{tx}(z)\le\sum_{z=1}^{|I|}E_i^{H}(z),\quad \forall i\in S. \tag{25}$$

Let Γ^{EH} be the minimum input power to the energy harvester of the IoT device to be able to harvest energy. Accordingly, IoT devices require that the received signal is greater that Γ^{EH} to enable them to harvest energy. Therefore,

$$\Gamma^{EH}H_{ei}(c,z)\le P_{ei}^{ET}(c,z)G_{ei}^{c},\quad \forall e\in ETS,\forall i\in S,\forall c\in\overline{C},z\in Z. \tag{26}$$

Furthermore, successful energy harvesting necessitates that the IoT device is located within an energy harvesting zone of an ET, i.e.,

$$H_{ei}(c,z)\le\mathbb{H}_{ei}^{c},\forall e\in ETS,i\in S,\forall c\in\overline{C},z\in Z. \tag{27}$$

Let BL_i^{init} and BL_i^{max} be initial and maximum battery level of the IoT device, respectively. Battery level of IoT device i during slot z, $BL_i(z)$, is defined as follows:

$$BL_i(1)=BL_i^{init},\quad \forall i\in S. \tag{28}$$

$$BL_i(z)=BL_i(z-1)-E_i^{tx}(z)+E_i^{H}(z)\quad \forall i\in S,z\in Z\setminus 1. \tag{29}$$

Since the battery level cannot exceed its maximum capacity or be negative, we have,

$$0\le BL_i(z)\le BL_i^{max}\quad \forall i\in S,z\in Z\setminus 1. \tag{30}$$

Moreover, the IoT device can transmit only if its battery level is not less than a certain threshold, BL^{min}. Hence,

$$X_i(c,z)\le\frac{BL_i(z)}{BL^{min}},\quad \forall i\in S,c\in C,z\in Z. \tag{31}$$

The objective is to minimize the total transmitted energy from all ETs. Therefore, we formulate the optimization problem as follows:

$$\mathbf{P1}:\mathbf{Minimize}:\sum_{e\in ETS}\sum_{i\in S}\sum_{c\in\overline{C}}\sum_{z=1}^{|I|}P_{ei}^{ET}(c,z)\ T \tag{32}$$

Subject to:

Constraints (6-21), (24-31).

$$X_i(c,z),X_{i,j}(c,z),H_i(\overline{c},z),H_{ei}(\overline{c},z)\in\{0,1\},\quad \forall i\in S,j\in\overline{S},e\in ETS,c\in C,\overline{c}\in\overline{C},z\in Z. \tag{33}$$

$$0\le f_{ij}^{y}(c,z)\le v,\ \forall i,j\in\overline{S},y\in d,c\in C,z\in Z. \tag{34}$$

$$0\le P_i^{tx}(c,z)\le P_{max}^{tx},\forall i\in S,c\in C,z\in Z. \tag{35}$$

$$0\le P_{ei}^{ET}(\overline{c},z)\le P_{max}^{ET},\quad \forall e\in ETS,i\in S,\overline{c}\in\overline{C},z\in Z. \tag{36}$$

IV. Generalized Benders Decomposition with Sequential Convex Programming (GBD-SCP)

In section III, the formulated problem is a Mixed Integer Nonlinear Program (MINLP), which is NP-Hard problem [8]. Moreover, the problem is considered non-convex MINLP, and there is no efficient method to solve the problem optimally. To facilitate finding a solution for the optimization problem, we first find a concave lower bound for equation (4) to approximate the data rate function. Then, we employ Successive Convex Programming (SCP) within Generalized Bender Decomposition (GBD) algorithm [9] to solve problem P1. In GBD, we decompose problem P1 into a Primal Problem (convex Non Linear Program (NLP)) and a Master Problem (Mixed Integer Linear Program (MILP)). Then, we solve these subproblems iteratively until converging to a certain solution.

To derive a concave lower bound for equation (4), we rewrite the data rate function as follows:

$$\begin{aligned}R_{ij}(c,z)&=W\log_2\Big(1+\frac{P_i^{tx}(c,z)\ G_{ij}^{c}}{\sum_{q\in S\setminus i}P_q^{tx}(c,z)\ G_{qj}^{c}+N_j}\Big)\\&=W\log_2\Big(\sum_{q\in S}P_q^{tx}(c,z)\ G_{qj}^{c}+N_j\Big)-\underbrace{W\log_2\Big(\sum_{q\in S\setminus i}P_q^{tx}(c,z)\ G_{qj}^{c}+N_j\Big)}_{\triangleq\hat{R}_{ij}(c,z)}\end{aligned} \tag{39}$$

Then, we find an upper bound for $\hat{R}_{ij}(c,z)$ using its first-order Taylor approximation around a point $\widetilde{P}_i(c,z)$ as follows:

$$\hat{R}_{ij}(c,z)\le W\log_2\Big(\sum_{q\in S\setminus i}\widetilde{P}_q(c,z)\ G_{qj}^{c}+N_j\Big)+\sum_{q\in S\setminus i}\frac{WG_{qj}^{c}\log_2(e)[P_i^{tx}(c,z)-\widetilde{P}_i(c,z)]}{[\sum_{r\in S\setminus i}\widetilde{P}_r(c,z)\ G_{rj}^{c}+N_j]}\triangleq\widetilde{R}_{ij}^{up}(c,z) \tag{40}$$

$$\mathcal{L}\Big(X_i(c,z), X_{ij}(c,z), H_i(\overline{c},z), H_{ei}(\overline{c},z), f_{ij}^{y(k)}(c,z), P_i^{tx(k)}(c,z), P_{ei}^{ET(k)}(\overline{c},z)\Big) = \sum_{\widetilde{e}\in ETS}\sum_{\widetilde{i}\in S}\sum_{\widetilde{c}\in C}\sum_{\widetilde{z}=1}^{|I|} P_{\widetilde{e}\widetilde{i}}^{ET(k)}(\widetilde{c},\widetilde{z})\ T +$$
$$\lambda^k(i,j,c,z)\Big(X_{ij}(c,z) - \sum_{q=1}^{|d|} f_{ij}^{q(k)}(c,z)\Big) + \Lambda^k(i,j,y,c,z)\Big(\tfrac{f_{ij}^{y(k)}(c,z)}{v} - X_{ij}(c,z)\Big) + \Theta^k(i,,z)\Big(X_i(c,z) - \tfrac{BL_i(z)^{(k)}}{BL^{min}}\Big) +$$
$$\Omega^k(e,i,\overline{c},z)\Big(P_{ei}^{ET(k)}(\overline{c},z) - P_{max}^{ET}\ H_{ei}(\overline{c},z)\Big) + \theta^k(i,j,y,c,z)\Big(f_{ij}^{y(k)}(c,z) - X_{ij}(c,z)\ \overline{R}_{ij}^{(k)}(c,z)\ T\Big) + \tag{37}$$
$$\omega^k(i,c,z)\Big(P_i^{tx(k)}(c,z) - P_{max}^{tx}X_i(c,z)\Big) + \psi^k(e,i,\overline{c},z)\Big(\Gamma^{EH}H_{ei}(\overline{c},z) - P_{ei}^{ET(k)}(\overline{c},z)G_{ei}^c\Big) +$$
$$\zeta^k(i,j,c,z)\Big(\Gamma X_{ij}(c,z)\big[\sum_{q\in S\setminus i} P_q^{tx(k)}(c,z)G_{qj}^c + \alpha_{ij}\big] - P_i^{tx(k)}(c,z)G_{ij}^c\Big).$$

$$\hat{\mathcal{L}}\Big(X_i(c,z), X_{ij}(c,z), H_i(\overline{c},z), H_{ei}(\overline{c},z), f_{ij}^{y(l)}(c,z), P_i^{tx(l)}(c,z), P_{ei}^{ET(l)}(\overline{c},z)\Big) = \hat{\lambda}^l(i,j,c,z)\Big(X_{ij}(c,z) - \textstyle\sum_{q=1}^{|d|} f_{ij}^{q(l)}(c,z)\Big)$$
$$+\hat{\Lambda}^l(i,j,y,c,z)\Big(\tfrac{f_{ij}^{y(l)}(c,z)}{v} - X_{ij}(c,z)\Big) + \hat{\Theta}^l(i,c,z)\Big(X_i(c,z) - \tfrac{BL_i(z)^{(l)}}{BL^{min}}\Big) + \hat{\Omega}^l(e,i,\overline{c},z)\Big(P_{ei}^{ET(l)}(\overline{c},z) - P_{max}^{ET}\ H_{ei}(\overline{c},z)\Big)$$
$$+\hat{\theta}^l(i,j,y,c,z)\Big(f_{ij}^{y(l)}(c,z) - X_{ij}(c,z)\ \overline{R}_{ij}^{(l)}(c,z)\ T\Big) + +\hat{\psi}^l(e,i,\overline{c},z)\Big(\Gamma^{EH}H_{ei}(\overline{c},z) - P_{ei}^{ET(l)}(\overline{c},z)G_{ei}^c\Big)$$
$$\hat{\omega}^l(i,c,z)\Big(P_i^{tx(l)}(c,z) - P_{max}^{tx}X_i(c,z) + \hat{\zeta}^l(i,j,c,z)\Big(\Gamma X_{ij}(c,z)\big[\textstyle\sum_{q\in S\setminus i} P_q^{tx(l)}(c,z)G_{qj}^c + \alpha_{ij}\big] - P_i^{tx(l)}(c,z)G_{ij}^c\Big)\Big). \tag{38}$$

From equation (40), we can approximate the data rate function by its concave lower bound, $\overline{R}_{ij}(c,z)$, as follows:

$$\overline{R}_{ij}(c,z) \triangleq W\log_2\Big(\sum_{q\in S} P_q^{tx}(c,z)G_{qj}^c + N_j\Big) - \widetilde{R}_{ij}^{up}(c,z) \tag{41}$$

Note: We use $+$ superscript on the binary variable in this paper to show that the binary variable value is fixed. In addition, we use (k) and (l) superscripts on the continuous variable to show that the continuous variable value is fixed after solving the primal and feasibility problems, respectively, in the k^{th} and l^{th} times, respectively.

A. Primal Problem

In the primal problem, we fix all binary variables and approximate the data rate function by its concave lower bound function, i.e. equation $\overline{R}_{ij}(c,z)$. The goal of solving the primal problem is to find an upper bound for the solution given by GBD-SCP algorithm. The resulting optimization problem is in a form of a convex NLP, and it is formulated as follows:

$$\mathbf{P2.1}: \mathbf{Minimize}:$$
$$\pi = \sum_{e\in ETS}\sum_{i\in S}\sum_{c\in\overline{C}}\sum_{z=1}^{|I|} P_{ei}^{ET}(c,z)\ T \tag{42}$$

Subject to:

Constraints (16-21), (25), (28-30) and (34-36).

$$X_{ij}^+(c,z) - \sum_{y=1}^{|d|} f_{ij}^y(c,z) \le 0, \quad \forall i\in S, j\in\overline{S}, c\in C, z\in Z. \tag{43}$$

$$\frac{f_{ij}^y(c,z)}{v} - X_{ij}^+(c,z) \le 0, \quad \forall i\in S, j\in\overline{S}, c\in C, y\in d, z\in Z. \tag{44}$$

$$P_i^{tx}(c,z) - P_{max}^{tx}X_i^+(c,z) \le 0,\ \forall i\in S, c\in C, z\in Z. \tag{45}$$

$$P_{ei}^{ET}(c,z) - P_{max}^{ET}\ H_i^+(c,z) \le 0, \quad \forall e\in ETS, i\in S, c\in\overline{C}, z\in Z. \tag{46}$$

$$f_{ij}^y(c,z) - X_{ij}^+(c,z)\ \overline{R}_{ij}(c,z)\ T \le 0, \quad \forall i\in S, j\in\overline{S}, y\in d, c\in C, z\in Z. \tag{47}$$

$$X_i^+(c,z) - \frac{BL_i(z)}{BL^{min}} \le 0, \forall i\in S, c\in C, z\in Z. \tag{48}$$

$$\Gamma\ X_{ij}^+(c,z)\big[\sum_{q\in S\setminus i} P_q^{tx}(c,z)\ G_{qj}^c + \alpha_{ij}\big] - P_i^{tx}(c,z)\ G_{ij}^c \le 0 \quad \forall i\in S, j\in\overline{S}, c\in C, z\in Z. \tag{49}$$

$$\Gamma^{EH}H_{ei}^+(c,z) - P_{ei}^{ET}(c,z)G_{ei}^c \le 0, \quad \forall e\in ETS, i\in S, c\in\overline{C}, z\in Z. \tag{50}$$

B. Feasibility Problem

The master problem uses Lagrange multipliers associated with the constraints (43-50) in the primal problem to get a lower bound for the solution of GBD-SCP algorithm. However, when the solution of the primal problem is not feasible, GBD-SCP uses Lagrange multipliers for the feasibility problem instead. Feasibility problem is similar to the primal problem except the following: 1) We introduce upper bound variables for the constraints associated with constraints (43-50) in the primal problem, and 2) The objective function for the feasibility problem is minimizing the summation of all these upper bound variables.

C. Master Problem

The goal of solving the master problem is to get a lower bound for the solution of GBD-SCP algorithm. In the master problem, we fix all continuous variables and solve the problem as an MILP. Let $\Phi^{(k)}$ and $\hat{\Phi}^{(l)}$ be the sets of Lagrange multipliers associated with the constraints (43-50) in the primal problem and the corresponding constraints in the feasibility problems, respectively, after solving them for the k^{th} and l^{th} times, respectively. Hence, $\Phi^{(k)}$ and $\hat{\Phi}^{(l)}$ are defined, respectively as follows: $\Phi^{(k)} = \{\lambda^k(i,j,c,z),\ \Lambda^k(i,j,y,c,z),\ \omega^k(i,c,z),\ \Omega^k(e,i,\overline{c},z),\ \theta^k(i,j,y,c,z),\ \Theta^k(i,c,z),\ \zeta^k(i,j,c,z),\ \psi^k(e,i,\overline{c},z)\}$, and $\Phi^{(l)} = \{\hat{\lambda}^l(i,j,c,z),\ \hat{\Lambda}^l(i,j,y,c,z),\ \hat{\omega}^l(i,c,z),\ \hat{\Omega}^l(e,i,\overline{c},z),\ \hat{\theta}^l(i,j,y,c,z),\ \hat{\Theta}^l(i,c,z),\ \hat{\zeta}^l(i,j,c,z),\ \hat{\psi}^l(e,i,\overline{c},z)\}, \forall i\in S, j\in\overline{S}, e\in ETS, y\in d, c\in C, \overline{c}\in\overline{C}, z\in Z, 1\le n\le k$. The support functions in equation (37) and (38) are defined in term of the aforementioned Lagrange multipliers and the binary variables. Hence, the master problem can be formulated to find a lower bound for GBD-SCP as follows:

$$\mathbf{P2.2}: \mathbf{Minimize}: \mu \tag{51}$$

Subject to:

Constraints (6), (9-12), (27), (33).

$$\mathcal{L}\Big(X_i(c,z), X_{ij}(c,z), H_i(\overline{c},z), H_{ei}(\overline{c},z), f_{ij}^{y(n)}(c,z), P_i^{tx(n)}(c,z), P_{ei}^{ET(n)}(\overline{c},z)\Big) \le \mu$$
$$\forall i\in S, j\in\overline{S}, e\in ETS, y\in d, c\in C, \overline{c}\in\overline{C}, z\in Z, 1\le n\le k. \tag{52}$$

$$\hat{\mathcal{L}}\Big(X_i(c,z), X_{ij}(c,z), H_i(\overline{c},z), H_{ei}(\overline{c},z), f_{ij}^{y(q)}(c,z), P_i^{tx(q)}(c,z), P_{ei}^{ET(q)}(\overline{c},z)\Big) \le 0$$
$$\forall i\in S, j\in\overline{S}, e\in ETS, y\in d, c\in C, \overline{c}\in\overline{C}, z\in Z, 1\le q\le l. \tag{53}$$

Algorithm 1: Generalized Benders Decomposition with Sequential Convex Programming (GBD-SCP)

1 Select initial fixed values for the binary variables and $\widetilde{P}_i(c,z)$, solve problem P2.1 successively using **Algorithm** 2, and let its solution and the corresponding Lagrange multipliers set be $\pi^{(1)}$ and $\Phi^{(1)}$, respectively.
2 Set $k=1$, $l=0$, $UB=\pi^{(1)}$.
3 Set $\widetilde{P}_i(c,z)=P_i^{tx*}(c,z)$ and fix all continuous variables.
4 Solve problem P2.2.
5 Let the solution of P2.2 be μ^*, and set $LB=\mu^*$.
6 **if** $(UB-LB)<\epsilon$ **then**
7 Terminate.
8 **else**
9 $\widetilde{P}_i(c,z)=P_i^{tx*}(c,z)X_i^*(c,z)$.
10 Fix all binary variables.
11 Solve problem P2.1 successively using **Algorithm** 2, and let the solution be $\pi^{(k)}$.
12 Find the Lagrange multipliers set, $\Phi^{(k)}$, if $\pi^{(k)}$ is feasible.
13 **if** ($\pi^{(k)}$ is feasible) **then**
14 $UB=\min(UB,\pi^{(k)})$.
15 **if** $(UB-LB)<\epsilon$ **then**
16 Terminate.
17 **else**
18 $k=k+1$. $\widetilde{P}_i(c,z)=P_i^{tx*}(c,z)$.
19 **else**
20 Solve the feasibility problem.
21 Find the Lagrange multipliers set, $\hat{\Phi}^{(l)}$.
22 $\widetilde{P}_i(c,z)=P_i^{tx*}(c,z)$, and fix all continuous variables.
23 $l=l+1$.
24 Go to step 4.

Algorithm 2: Sequential Convex Programming (SCP)

1 $r=1$, $\Pi^{(0)}=\infty$
2 **while** ($r\neq$ Max iterations) **do**
3 Solve problem P2.1, and let its solution be $\Pi^{(r)}$.
4 **if** (The solution is feasible) **then**
5 **if** $(\Pi^{(r-1)}-\Pi^{(r)}>\delta)$ **then**
6 Let $\widetilde{P}_i(c,z)=P_i^{tx*}(c,z)$ and $r=r+1$.
7 **else**
8 Set $\pi^{(k)}=\Pi^{(r)}$ and terminate.
9 **else**
10 Terminate.

D. GBD-SCP Algorithm Description

Algorithm 1 shows the steps used to solve the optimization problem iteratively using GBD and SCP. First, we select initial values for the binary variables and $\widetilde{P}_i(c,z)$, then GBD-SCP solves the primal problem using SCP which is described in Algorithm 2. Without loss of generality, we assume that we can find initial values of the binary variables that lead to a feasible solution for problem P2.1. We solve a problem that minimizes the sum of the binary variables subject to all linear constraints in problem P1 that are related to the binary and flow variables. Then, we select the solutions of the binary variables as initial values for the binary variables in GBD-SCP algorithm. Moreover, the initial value of $\widetilde{P}_i(c,z)$ is the maximum transmission power. Accordingly, GBD-SCP finds the solution of problem P2.1, $\pi^{(1)}$, and the corresponding Lagrange multipliers set $\Phi^{(1)}$. If we cannot find initial values that lead to a feasible solution for the primal problem, then we need to solve the feasibility problem after that to get the Lagrange multipliers set $\hat{\Phi}^{(1)}$ and increase l counter by 1.

GBD-SCP initializes the counters k and l and the upper bound UB as shown in step 2. In steps 3-4, GBD-SCP updates the value of $\widetilde{P}_i(c,z)$, fixes the continuous variables and solves problem P2.2. In steps 5-10, GBD-SCP selects the solution of P2.2 as a lower bound, LB, and it terminates if the difference between UB and LB is less than ϵ. Otherwise, GBD-SCP updates $\widetilde{P}_i(c,z)$ and fixes all binary variables.

In steps 11-12, GBD-SCP solves P2.1 using SCP, and hence, find the Lagrange multipliers set $\Phi^{(k)}$ and the solution of P2.1, $\pi^{(k)}$. If the solution of P2.1 is feasible, GBD-SCP updates the upper bound value as shown in steps 11-12. In steps 15-18, GBD-SCP increases the counter k and updates the value of $\widetilde{P}_i(c,z)$ if the difference between UB and LB is greater than or equal to ϵ, and it terminates otherwise. If the solution of P2.1 is not feasible, GBD-SCP solves the feasibility problem to find the Lagrange multipliers set $\hat{\Phi}^{(l)}$ as shown in steps 20-21. Then, it updates $\widetilde{P}_i(c,z)$, fixes the continuous variables and increases the counter l in steps 22-23. The algorithm iterates until the termination condition is met. It is shown in [9] that GBD algorithm terminates in a finite number of steps.

V. Simulation Results

In this section, we present simulation results for our proposed work to minimize total transmitted energy for ETs to IoT devices in cellular networks. We use SCIP [10], IPOPT [11] and CPLEX [12] under (GAMS) [13] to solve problems P1, P2 and P3, respectively. SCIP employs a spatial branch-and-bound algorithm to solve convex and non-convex MINLP optimally [10]. Cellular and Iot devices are uniformly distributed, and we use two network sizes in the simulation. Unless specified otherwise, the network sizes are: 1) Small network: consists of 9 ETs operating over 2 channels, 10 IoT and 5 cellular devices operating over 2 channels and 3 destinations for the multicast session and 2) Large network: consists of 25 ETs operating over 5 channels, 15 IoT and 8 cellular devices operation over 5 channels and 5 destinations for the multicast session.

We compare the performance of GBD-SCP with optimal solution when the network size is small due to difficulty of obtaining the optimal solution when the number of variables is very large. The ETs are located within 100 meters of the BS as assumed in [3]. The multipath fading is exponentially distributed with unit mean. Moreover, the distribution of the shadowing is log-normal standard deviation of 8 dB. Table I shows the rest of the simulation parameters.

TABLE I: Simulation Parameters

Parameter	Value	Parameter	Value
PL_c	0.01	N_0	-174 dbm/Hz
PL_e	2	BL^{min}	10 mAh
P^{ET}_{max}	20 W	BL_i^{init}	300 mAh
P^{BS}	20 W	BL_i^{max}	500 mAh
W	6 MHz	$\underline{\phi}$	15°
η	0.652	$\overline{\phi}$	20°
v	1 Mb	Γ	10
P^{tx}_{max}	250 mW	Γ^{cell}	10
T	0.1 sec	ϵ	0.01
Γ^{EH}	-21 dBm	δ	0.01

Table II shows the total transmitted energy from all ETs and the computation time for the optimal and GBD-SCP algorithm. When the network size is small, the performance of GBD-SCP is close to the optimal in term of total transmitted energy. On the other hand, there is no efficient way to obtain the optimal solution when the network size is large since the computational complexity increases rapidly by increasing the number of variables. It is shown that the total transmitted energy when the network size is large is less that the total transmitted energy when the network size is small. The reason

for that is the number of ETs in the large network size is greater than the number of ETs in the small network size. We show in the section the positive effect of increasing the number of ETs in the amount of the total transmitted energy.

TABLE II: GBD-SCP algorithm performance

	Transmitted Energy		Computation Time	
Network size	Optimal	GBD-SCP	Optimal	GBD-SCP
Small	0.711	0.72	443	8.89
Large	N/A	0.256	N/A	874

Table II shows also the computation times when we solve the problem optimally and when we use GBD-SCP algorithm for both small and large networks. For small network size, it is shown that GBD-SCP algorithm reduces the computation time significantly. This is due to approximating the non-convex data rate function and decomposing the problem into a convex NLP and an MILP subproblems. Furthermore, the computation time for GBD-SCP increases when the network size is large. This increase in time is due to the rapid increase in the number of variables, and that leads to more computation time requirement. On the other hand, there is no efficient way to obtain the optimal solution for the MINLP problem when the network size is large due to the increase in the number of variables. However, GBD-SCP can provide solutions for large network size since the primal problem is convex and the master problem is an MILP which can be solved efficiently using CPLEX solver.

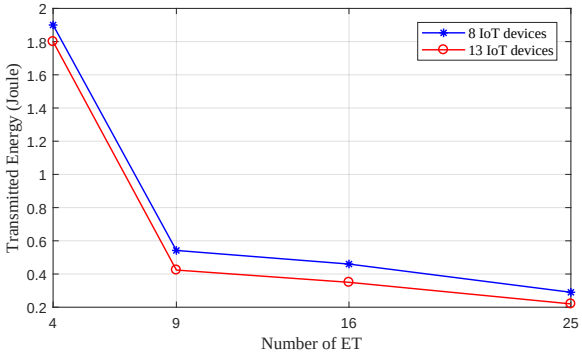

Fig. 2: Transmitted energy vs number of ETs.

Fig. 2 shows the total transmitted energy when GBD-SCP algorithm is used and the number of channels, cellular devices and destinations are 4, 7 and 5, respectively. It is shown how the total transmitted energy is related to the number of ETs in the network. The total transmitted energy by all ETs in the network decreases significantly when the number of ETs increases. The reason is that increasing the number of ETs can help the IoT devices to receive energy from ETs with better channels conditions. Hence, the total transmitted energy is reduced while satisfying the energy demands for the IoT devices. On the other hand, the transmitting IoT can forward the multicast message through the base station or through another IoT to the destination. When the channel condition to a neighboring IoT is better than the channel condition to the base station, the IoT can select forwarding the multicast message through the neighboring IoT if that leads to minimizing the energy used for transmission. Accordingly, the total transmitted energy to the transmitting IoT can be reduced. Since increasing the number of IoT devices in the network increases the possibility of forwarding the multicast message through neighboring IoT devices with better channel conditions, this can lead to reducing the consumed energy for transmission, and hence, reducing the total transmitted energy by ETs as shown in Fig. 2 .

Fig. 3 shows total transmitted energy versus the number of multicast destinations in the network when the number of channels, cellular devices and ETs are 4, 3 and 25, respectively. Increasing the number of destinations can lead to more IoT devices engaging in forwarding the multicast messages, and hence, more energy consumption for

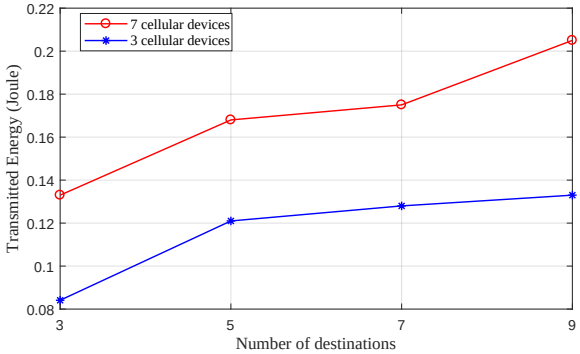

Fig. 3: Transmitted energy vs number of destinations.

multicast message transmission. Therefore, ETs tend to transfer more energy to the IoT devices when the number of multicast destinations increases as shown in Fig. 3. Increasing the number of cellular users can lead to more interference to the receiving IoT devices. Therefore, the transmitting IoT may require more energy for data transmission. Accordingly, the ETs transmit more energy to the IoT devices to satisfy their energy demands.

VI. Conclusion

In this paper, we considered energy harvesting-based multicast communication in cellular IoT. We proposed to wirelessly power the IoT multicast communication to encourage the IoT device to participate in forwarding the multicast messages while not depleting their battery in collaboration. Our formulated problem is a non-convex MINLP, where there is no efficient way to solve it in general. The data rate function is non-convex, and hence, we approximate it with a concave lower bound function. Then, we utilized GBD algorithm with SCP to decompose the optimization problem into a convex NLP and a MILP subproblems. We evaluated the performance of GBD-SCP algorithm and we showed that it achieves a performance close to the optimal while the computation time is reduced significantly.

References

[1] D. Lecompte and F. Gabin, "Evolved Multimedia Broadcast/Multicast Service (eMBMS) in LTE-Advanced: Overview and Rel-11 Enhancements," IEEE Commun. Mag., vol. 50, no. 11, Nov. 2012, pp. 68-74.

[2] A. Al-Fuqaha and et al., "Internet of things: A survey on enabling technologies protocols and applications", IEEE Commun. Surveys Tuts., vol. 17, no. 4, pp. 2347-2376, 2015.

[3] H. Tabassum and et al., "Wireless-powered cellular networks: Key challenges and solution techniques," IEEE Commun. Mag., vol. 53, no. 6, pp. 63-71, Jun. 2015.

[4] A. Almasoud and A. E. Kamal, "Efficient Data and Energy Transfer in IoT with a Mobile Cognitive Base Station", in the proceedings of IEEE PIMRC, 2017, pp. 1-5.

[5] F. Yuan, Q. T. Zhang, S. Jin, and H. Zhu, "Optimal harvest-use-store strategy for energy harvesting wireless systems," IEEE Trans. Wireless Commun., vol. 14, no. 2, pp. 698710, Feb. 2015.

[6] A. Ercan, O. Sunay, and I. F. Akyildiz, "RF energy harvesting and transfer for spectrum sharing cellular IoT communications in 5G systems," IEEE Trans. Mobile Comput., to be published.

[7] C. A. Balanis, "Antenna Theory: Analysis and Design," New Jersey: John Wiley & Sons, 2005, p. 68.

[8] M. R. Garey and D. S. Johnson, "Computers and Intractability: A Guide to the Theory of NP-Completeness," New York: Freeman, 1979.

[9] A. M. Geoffrion, "Generalized benders decomposition," J. Optim. Theory Applicat., vol. 10, pp. 237-260, 1972.

[10] S. Vigerske and A. Gleixner, "SCIP: Global optimization of mixedinteger nonlinear programs in a branch-and-cut framework," Zuse Institute Berlin, Berlin, Germany, Rep. 16-24, 2016.

[11] A. Wchter and L. T. Biegler, "On the implementation of an interiorpoint filter line-search algorithm for large-scale nonlinear programming," Math. Program., vol. 106, pp. 25-57, May 2006.

[12] A. Brooke, D. Kendrick, A. Meeraus, and R. Raman, GAMS/Cplex 7.0 User Notes. Washington, DC: GAMS Development Corp., 2000.

[13] R. Rosenthal, GAMS A Users Guide, Washington, DC, USA, GAMS Development Corporation, 2007.